

## COMMUNICATION


 CrossMark  
 click for updates
Cite this: *Soft Matter*, 2015, 11, 850Received 8th November 2014  
Accepted 17th December 2014

DOI: 10.1039/c4sm02480j

www.rsc.org/softmatter

## On the structure of the $N_x$ phase of symmetric dimers: inferences from NMR†

Anke Hoffmann,<sup>a</sup> Alexandros G. Vanakaras,<sup>\*b</sup> Alexandra Kohlmeier,<sup>c</sup> Georg H. Mehl<sup>c</sup> and Demetri J. Photinos<sup>b</sup>

NMR measurements on a selectively deuterated liquid crystal dimer CB-C9-CB, exhibiting two nematic phases, show that the molecules in the lower temperature nematic phase,  $N_x$ , experience a chiral environment and are ordered about a uniformly oriented director throughout the macroscopic sample. The results are contrasted with previous interpretations that suggested a twist-bend spatial variation of the director. A structural picture is proposed wherein the molecules are packed into highly correlated chiral assemblies.

The classical nematic phase (N) with only orientational ordering of the molecules is theoretically and experimentally the LC phase which, due to its structural simplicity and technological importance, is by far the most investigated and best understood of all LC phases.<sup>1</sup> Thus the detection of LCs forming two nematic phases is of very high interest, as such observations pose the challenge to test and recalibrate fundamental concepts of LC phase behaviour. Direct transitions between two uniaxial thermotropic nematic phases are typically associated with the formation of more complex molecular aggregates in the low temperature nematic phase, such as column formation in the transition to the columnar nematic phase<sup>2</sup> of discotic or bent core materials.<sup>3</sup> For main chain LCPs, examples have been reported where a first order phase transition can occur between two nematic phases.<sup>4</sup>

The recent observation of an additional, low temperature, nematic phase, initially termed  $N_x$ ,<sup>5,6</sup> and more recently  $N_{tb}$ , in cyanobiphenyl based dimers with positive dielectric anisotropy, where the mesogens are separated by odd-numbered hydrocarbon spacers,<sup>5–12</sup> and in specifically prepared difluoro-terphenyl mesogens<sup>11</sup> with negative dielectric anisotropy, as

well as in non-symmetric dimers,<sup>13</sup> has sparked a rapidly increasing interest in this class of LCs, and particularly in the structure of this new nematic phase in thin films and in the bulk. These LCs exhibit characteristic periodic stripe patterns and rope textures in thin films and an electro-optical response typically found in chiral systems, though the molecules are non-chiral.<sup>6,10,11,14</sup> XRD investigations show clearly the absence of layer reflections, confirmed by extensive miscibility calorimetric studies.<sup>5</sup> The presence of stripes and Bouligand arches with periodicities in the 8–10 nm regime in freeze fracture TEM<sup>12</sup> images was interpreted as formation of chiral structures on surfaces, however, recent evidence based on AFM studies might suggest that these features could be artefacts due to the onset of surface crystallisation.<sup>15</sup> Lastly, in a series of papers<sup>8,9,16</sup> focused on an extensive NMR characterization of CB-C7-CB it is argued that the interpretation of the NMR measurements is consistent with a helicoidal conical (“heliconal”) nematic phase wherein the spatial distribution of the nematic director is  $\mathbf{n}(Z) = (\sin \theta_0 \cos kZ, \sin \theta_0 \sin kZ, \cos \theta_0)$ , defining a conical helix of constant pitch  $2\pi/k$  and constant “tilt” angle  $\theta_0$  between  $\mathbf{n}$  and the helix axis  $Z$ . Whilst this is in line with a spontaneous twist-bend elastic deformation predicted<sup>17</sup> for the nematic phases of achiral banana-shaped molecules, it should be stressed that the structural periodicity of 8–10 nm observed in the  $N_x$  phase of dimers<sup>11,12</sup> cannot be readily identified with the periodicity implied by the theoretical proposals of the “twist-bend” nematic phase.<sup>17</sup> Such proposals are based on the continuum theory of elasticity for the nematic phase, involving the elementary (twist, bend, splay) deformations according to the Frank-Oseen formulation of the elastic free energy. However, the validity of the fundamental assumptions of the continuum theory concerning the slow variations of the director field<sup>1</sup> is problematic when the macroscopic director supposedly undergoes a reorientation of  $2\theta_0$  over the distance of a half-pitch, which might be as short as one or two molecular lengths. In an attempt to by-pass this inconsistency, the notion of the “half-molecular director”, representing the local average orientation of the long axis of a biphenyl half-molecular core, is introduced<sup>12</sup> in place

<sup>a</sup>Department of Inorganic and Analytical Chemistry, University of Freiburg, Albertstr. 21, 79104 Freiburg, Germany

<sup>b</sup>Department of Materials Science, University of Patras, Patras 26504, Greece. E-mail: a.g.vanakaras@upatras.gr

<sup>c</sup>Department of Chemistry, University of Hull, Hull, HU6 7RX, UK

† Electronic supplementary information (ESI) available. See DOI: 10.1039/c4sm02480j

of the macroscopic nematic director  $\mathbf{n}(Z)$ . Computer simulations, on the other hand, are not subject to the small length-scale restrictions of continuum models and there it is found that bent core molecules with flexible arms,<sup>18</sup> a model bearing structural analogies with the odd-spacer dimers, can form nematic phases consisting of chiral domains which spontaneously self-assemble into larger helical structures. Notably, chiral domains in the nematic phase of achiral compounds exhibiting dimerisation through hydrogen bonding were reported more than 15 years ago;<sup>19</sup> however, such domains were found to exhibit macroscopic twist deformation of the director in the optical regime. Lastly, although the twist-bend model has been proposed<sup>8,9,11,12,16,20</sup> for the consistent interpretation of various experimental observations on the dimer  $N_x$  phase, there is, to our knowledge, no direct identification of the helical structure and, furthermore, there are indications<sup>21,22</sup> that the dominant molecular arrangement in the  $N_x$  phase could differ from that of the twist-bend model.

In this communication we show, based on NMR studies of a selectively deuterated material of the structure CB-C9-CB presented in Fig. 1a (preparation details are given in ESI-4† (ref. 23)), that the helicoidal conical structure is not identified as the organisation of the  $N_x$  phase in the bulk.

The phase sequence of this statistically achiral compound is as follows. Heating: Cr 83.9  $N_x$  106.5 N 122.7 Iso ( $^{\circ}\text{C}$ ); cooling:

Iso122.1 N 106.4  $N_x$  48.5 Cr ( $^{\circ}\text{C}$ ). The sequence is determined by DSC at  $10\text{ }^{\circ}\text{C min}^{-1}$  (see ESI-5† (ref. 23)) and is close to that of non-deuterated CB-C9-CB for which the  $N_x$  phase was observed first<sup>5</sup> and to CB-C7-CB.<sup>8</sup> The materials in the N phase are typical, relatively viscous, uniaxial nematics. The onset, through a first order phase transition, of the low temperature  $N_x$  phase is accompanied by a significant increase of the viscosity (see also ESI-2† (ref. 23)).

Fig. 1(b and c) show the quadrupolar spectra of aligned CB-C9-CB in the temperature range from 110–80  $^{\circ}\text{C}$ . The line shape and the width of the peaks suggest that the sample is uniformly oriented along the magnetic field of the spectrometer (for experimental details see ESI-1† in (ref. 23)).

In terms of  $^2\text{H-NMR}$  analysis, the characteristic feature of the N- $N_x$  phase transition is the onset of the doubling of the quadrupolar peaks of the  $\text{CD}_2$  sites (Fig. 1(b and c)). Specifically, on entering the  $N_x$  range, each of the spectral lines of the  $\alpha\text{-CD}_2$  groups splits into two lines with splittings  $\Delta\nu_1$  and  $\Delta\nu_2$ , of essentially equal integrated intensity (see ESI-1.2† (ref. 23)) and with continuously increasing separation with decreasing temperature. The quantity  $\Delta\nu = (\Delta\nu_1 + \Delta\nu_2)/2$  is insensitive to temperature, with only a slight increment on cooling; see Fig. 2c. The onset of the peak doubling appears, at the resolution of the NMR experiment, to be nearly continuous. However, this does not necessarily indicate a continuous phase transition because the intrinsic width of the double peaks is comparable to their separation near the transition temperature and this does not allow a definite distinction between a strictly continuous transition and a weak first order transition (which applies to the present case according to calorimetry measurements<sup>23</sup>).

While this peak-doubling alone does not allow us to directly single out a particular underlying mechanism among several possibilities, the mechanism of loss of equivalence of the two deuterated sites<sup>24</sup> as a result of the onset of local chiral asymmetry in the  $N_x$  phase is strongly supported by the detailed NMR studies in (ref. 8 and 9) on CB-C7-CB together with other results<sup>25</sup> which suggest the presence of chiral asymmetry. Accordingly, our analysis and interpretation of the present data is based on adopting the hypothesis of the onset of local chiral asymmetry in the  $N_x$  phase on a longer time scale than the time-averaging inherently involved in the NMR measurement. Within this interpretation, the intensities of the two sub-peaks should be strictly equal as they correspond to equal numbers of (orientationally inequivalent) deuterated sites. Also, since the individual dimer molecules are statistically achiral, it is expected that a chirally unbiased bulk sample should consist of domains exhibiting both senses of chirality and with equal molecular populations for either sense. It should be noted that in the present work, in contrast to the assumptions in (ref. 8, 9, 16 and 20), the origin of the chirality is not necessarily attributed to the twist-bend deformation of the director. In fact it is shown here that such deformation is not implied by the NMR measurements and, moreover, that a number of additional assumptions, of questionable validity, would need to be invoked in order to make the assumed presence of the twist-bend deformation compatible with these measurements.

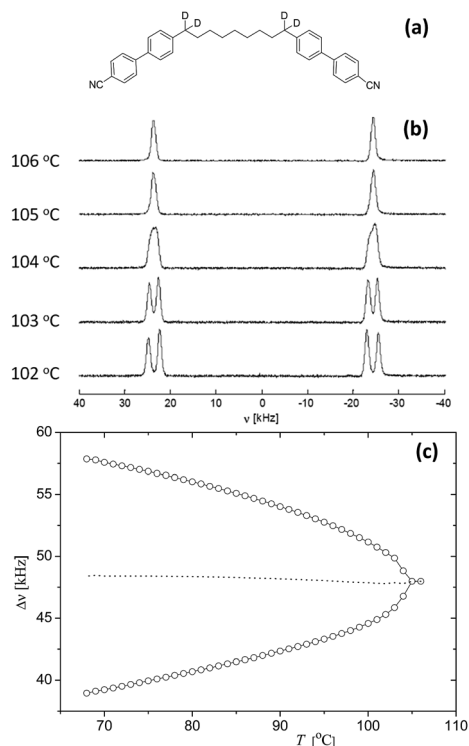
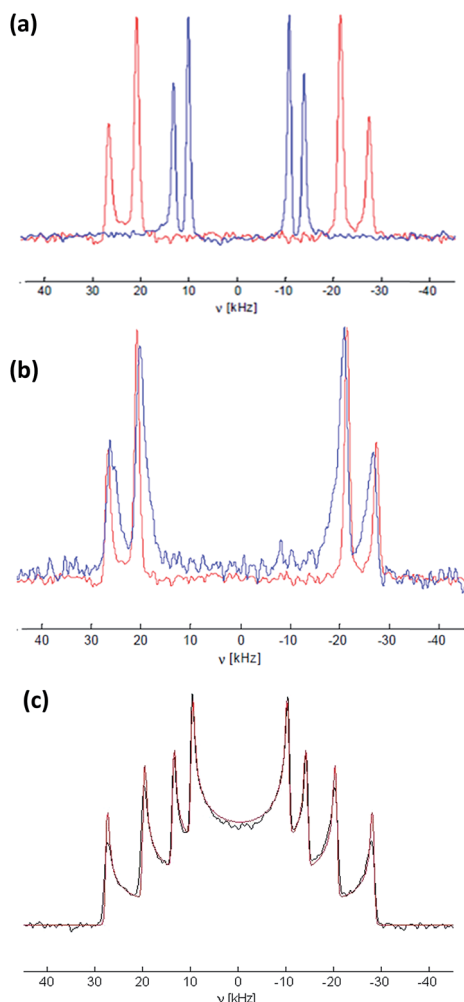


Fig. 1 (a) Structure of the deuterated molecule CB-C9-CB, ( $\alpha,\omega$ -bis(4,4'-cyanobiphenyl) nonane-(1,1,9,9-d<sub>4</sub>)). (b) Measured  $^2\text{H}$  NMR spectra recorded close to the N- $N_x$  phase transitions (cooling run). (c) The dependence of the measured quadrupolar splittings,  $\Delta\nu$ , on the temperature  $T$  for the 1,9 deuterons. The dotted line represents the mean value of the two splittings.



**Fig. 2** (a)  $^2\text{H}$  NMR spectra of the aligned sample (red) and after a flip by  $90^\circ$  with respect to the magnetic field (blue) in the  $N_x$  phase at  $90^\circ\text{C}$ . (b)  $^2\text{H}$  NMR spectrum 10 s after the  $90^\circ$  flip (blue); the red line corresponds to the initial spectrum in the  $N_x$  phase at  $90^\circ\text{C}$ . (c) Spinning sample (100 rpm)  $^2\text{H}$  NMR spectrum in the  $N_x$  phase at  $80^\circ\text{C}$ .

The measured splitting in the quadrupolar spectrum of the  $\alpha\text{-CD}_2$  group in the nematic phase is related to the respective orientational order parameter  $S_{\alpha\text{-CD}}^{(H)} = \langle P_2(\hat{\mathbf{e}}_{\alpha\text{-CD}} \cdot \hat{\mathbf{H}}) \rangle$  according to  $\Delta\nu = 3/2 |q_{\text{CD}} S_{\alpha\text{-CD}}|$ , with  $\hat{\mathbf{e}}_{\alpha\text{-CD}}$  denoting the orientation of the CD bond,  $\hat{\mathbf{H}}$  the direction of the spectrometer magnetic field, the superscript (H) indicating that the order parameter is evaluated relative to that direction,  $q_{\text{CD}}$  the quadrupolar coupling constant (here set at the value of 168 kHz),  $P_2$  the second Legendre polynomial and the angular brackets indicate ensemble time-averaging.<sup>26</sup> From the quadrupolar spectrum of the  $\alpha\text{-CD}_2$  group in the high temperature N phase (Fig. 1b) at  $106^\circ\text{C}$ , with a splitting of  $\Delta\nu \approx 48$  kHz, we obtain the value of  $-0.19$  for  $S_{\alpha\text{-CD}}^{(H)}$ . The order parameter of the mesogenic core unit  $S_{\text{core}}^{(H)} = \langle P_2(\hat{\mathbf{e}}_p \cdot \hat{\mathbf{H}}) \rangle$ , with  $\hat{\mathbf{e}}_p$  denoting the unit vector along the *para*-axis of the cyanobiphenyl unit, is related to  $S_{\alpha\text{-CD}}^{(H)}$  according to  $S_{\alpha\text{-CD}}^{(H)} = S_{\text{core}}^{(H)} P_2(\hat{\mathbf{e}}_p \cdot \hat{\mathbf{e}}_{\alpha\text{-CD}})$ . Assuming a fixed tetrahedral angle of the  $\alpha\text{-CD}$  bonds relative to the *para*-axis of the cyanobiphenyl mesogenic core, we obtain for  $S_{\text{core}}^{(H)}$  the value

0.57; this falls within the typical range for nematics. In the low temperature  $N_x$  phase,  $S_{\text{core}}^{(H)}$ , obtained analogously from  $\Delta\nu$ , shows only a slight further increase on cooling and appears to saturate at the value of 0.6. It is noted here that the order parameter  $S_{\text{core}}^{(H)}$  quantifies the orientational ordering of the mesogenic cores relative to the magnetic field. In a locally uniaxial nematic phase, the direction of maximal orientational ordering defines the local director  $\mathbf{n}$  and the respective order parameter, here denoted by  $S_{\text{core}}^{(n)}$ , is related to the experimentally accessible  $S_{\text{core}}^{(H)}$  according to  $S_{\text{core}}^{(H)} = S_{\text{core}}^{(n)} P_2(\mathbf{n} \cdot \mathbf{H})$ .

The crucial NMR experiment for testing the formation of the helicoidal conical structure in the bulk makes use of the high viscosity of the  $N_x$  phase. This allows collection of NMR spectra with the sample oriented perpendicular to the magnetic field. Specifically, when rotating the initially aligned sample to  $90^\circ$  with respect to the magnetic field, there is sufficient time to measure the NMR spectrum in this configuration before the magnetic field reorients the sample. Fig. 2a shows the quadrupolar spectrum at  $90^\circ\text{C}$  before (red) and after (blue) a rotation of the sample by  $90^\circ$  with respect to the magnetic field. The spectrum of the flipped sample measured 10 s after the flip (blue in Fig. 2b) shows essentially identical splittings with the initial spectrum (red) but is still not fully relaxed back along the direction of  $\mathbf{H}$  within this time interval. From the spectra in Fig. 2a we observe that the  $90^\circ$  flipped sample (i) does not exhibit any line broadening, the line shape being the same as the initially aligned sample, in fact with some slight narrowing and (ii) the quadrupolar peaks are essentially at half the initial splitting. Moreover, the spinning sample patterns of Fig. 2c are typical of a cylindrical distribution of the director about the axis of spinning.

These results have immediate implications on the structures possible for the  $N_x$  phase. First, there is no indication of the helicoidal structure. Secondly, the presence of such structure appears to be directly contradicted by the  $90^\circ$ -flip and the spinning sample spectra. The configuration of the nematic director for this hypothetical structure is given in Fig. 3a for the magnetically aligned sample. With the helix axis aligning parallel to the external magnetic field, the director makes a fixed angle  $\theta_{n,H} = \theta_0$  with the field. In such a distribution of the

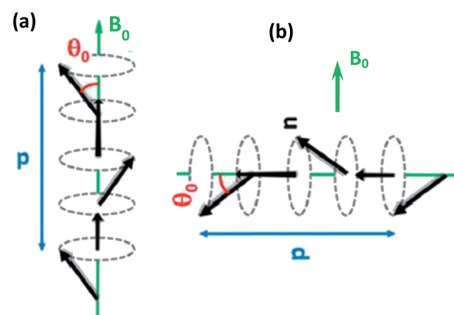


**Fig. 3** Schematic representation of the hypothetical (not supported by the present findings) helicoidal configuration of the nematic director for (a) the magnetically aligned sample<sup>16</sup> and (b) the sample rotated by  $90^\circ$  relative to the magnetic field.

director, rotating the sample by  $90^\circ$  about an axis perpendicular to the magnetic field generates a distribution of angles,  $\theta_{n,H}$ , in the range  $\pi/2 - \theta_0 < \theta_{n,H} < \pi/2 + \theta_0$ , whose breadth increases with increasing  $\theta_0$ . Accordingly, a direct indication of the presence of a heliconical configuration of the director would be a spectrum consisting of the superposition of peaks corresponding to the continuous distribution of the  $\theta_{n,H}$  angle over the above range. No sign of such distribution is detected in the measured spectra of Fig. 2a. Instead, a spectrum typical of the rotation of a uniformly distributed director, from parallel to perpendicular orientation relative to the magnetic field, is seen. The combined resolution of the experimental measurement and spectral fitting procedure for the detection of fluctuations of the  $\theta_{n,H}$  angle is  $5^\circ$  (see ESI-3.1† (ref. 23)). At this level of resolution, the  $90^\circ$ -rotated and the spinning sample spectra clearly indicate that the twist-bend helical configuration of the director, either throughout the sample or in domains of opposite handedness, is not observed in the  $N_x$  phase.

Could the twist-bend configuration of the director be present but escape detection by the present experiments? Two possibilities could be readily considered:

(i) One possibility would be if the hypothetical twist-bend has a very small value of the “tilt” angle  $\theta_0$ , *i.e.* below the resolution threshold of  $5^\circ$ . However, this would be well below the reported estimates for  $\theta_0$  from various experimental and theoretical considerations<sup>8,9,12,16</sup> which place it in the range  $10^\circ < \theta_0 < 38^\circ$ . Moreover, according to the twist-bend model,<sup>17</sup> the free energy contributions of the twist and bend deformations are proportional to  $k^2\theta_0^2$  and  $k^2\theta_0^4$  respectively; therefore a marginal value of  $\theta_0$  would correspond to marginal twist (as well as bend) which is not in accordance with the measured effects of chirality on the NMR spectra.

(ii) A second possibility would be to assume that the translational diffusion of entire dimer molecules along the hypothetical helix axis over distances of one pitch length is rapid on the NMR time scale (in this case  $10^{-4}$  s); then the time-averaged molecular motions, by sampling different orientations of the heliconically distributed director, would produce an effectively uniaxial spectrum about the helix axis. The assumed rapid diffusion should extend only within domains of a given chirality and be slow across domains of the opposite chirality in order to preserve the observed doubling of the splittings. To our knowledge there is no quantitative evidence to directly prove or disprove such assumptions. Furthermore, it is not clear how the assumed combination of rapid/slow diffusion would come about in a positionally disordered phase and how it would be in accordance with the observed dramatic increase of the rotational viscosity in the  $N_x$  phase. However, if such assumption is proven valid it would simply mean that the NMR techniques used here and in (ref. 8, 9 and 16), are “blind” to the possible presence of a heliconical twist-bend structure of the director in the  $N_x$  phase.

Apart from the absence of any indication of a twist-bend structure, the following can be inferred from the spectra in Fig. 1 and 2:

(a) The chiral domains in the  $N_x$  sample exhibit molecular orientational ordering along a unique direction (the local director of the domain) which aligns parallel to the magnetic field, as shown schematically in Fig. 4, middle.

(b) Rotating the  $N_x$  sample about the magnetic field preserves the collective mutual alignment of the domains (Fig. 4, right) sufficiently long ( $\sim 1$  s) on the NMR time scale ( $\sim 10^{-4}$  s) before relaxing back along the magnetic field.

(c) The complete separation of each peak into two sub-peaks (*i.e.* with marginal intensity between the two sub-peaks), exhibited by the measured spectra toward the low temperature end of the  $N_x$  phase (see Fig. 1b), indicates that the sample consists entirely of chiral domains, with practically no achiral regions which could be detected within the experimental resolution of the measurements. This would imply that the “volume over surface-area” of the domains is large, rendering the number of molecules in the domain interface negligible in comparison with the molecules in the domain interior.

(d) At higher temperatures in the  $N_x$  phase, the sub-peaks are overlapping and it cannot be excluded that part of the intensity might correspond to a substantial achiral contribution whose extent, however, cannot be directly estimated from the spectra.

As the NMR technique used is not sensitive to the distribution of molecular positions and the data presented here are from just the deuterated termini of the dimer spacer, no firm inferences can be drawn on the detailed molecular organization within the chiral domains of the  $N_x$  phase. An extensive consideration of the possible structures is undertaken in a forthcoming communication<sup>27</sup> based on a wide set of available observations. On the other hand, combining the present results with existing knowledge of the conformational statistics of the CB-C9-CB dimers<sup>26,28,29</sup> and their packing in the solid phase,<sup>30</sup> a general picture could be proposed where the dimer molecules within these domains assume predominantly twisted, chiral conformations<sup>26</sup> and the enantio-selective local molecular packing confers to the domain its chirality. This picture is in accordance with a periodicity of 9 nm of the twist found in crystalline samples<sup>30</sup> and in similar systems, where TEM data indicate periodicities of 8 nm (ref. 12), as well as with structures identified in recent AFM and FFTEM observations<sup>22</sup> in thin

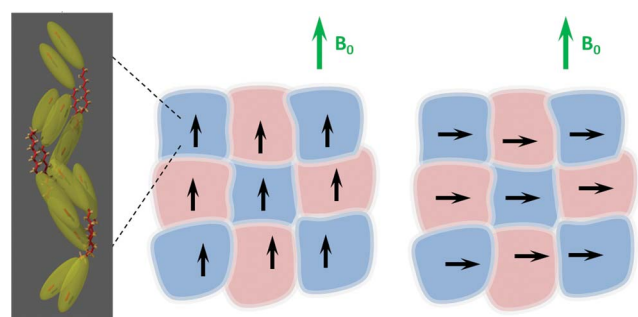


Fig. 4 Proposed chiral domain structure of the  $N_x$  phase. The different domain colors indicate opposite chiralities (sense of molecular twisting). The inset (left) shows a possible disposition of the mesogenic units within each domain, stressing the lack of full alignment of all the units parallel to a unique direction. The internal orientational order of each domain is represented by a domain director. The magnetic field aligns the domain directors (middle). On rotating the sample (right), the mutual alignment of the domain directors persists sufficiently long on the NMR measurement time-scale.

films. It should be noted here that these periodicities do not reflect any ordering of the molecular positions within the chiral domains of the  $N_x$  phase as these domains show only the short-range positional correlations associated with the local molecular packing of the bent conformations (see Fig. 4, left). The chiral domain picture is also consistent with the dramatic increase of the viscosity on going from the N to the  $N_x$  phase, as the reorientation processes in the latter would involve the rotation of domains of strongly correlated molecules. Lastly, it readily accounts for the experimental observation that the ordering of the mesogenic units along the magnetic field remains relatively low (0.5 to 0.6) throughout the  $N_x$  range. Specifically, the mesogenic units of the dimers, due to the statistical dominance of nonlinear conformations, cannot attain a simultaneous alignment along any given direction ("orientational frustration", see Fig. 4, left). Accordingly, though a direction of maximal alignment (*i.e.* the local director) can be uniquely defined, within each domain, and for the entire aligned sample, the respective value of the order parameter is low. This is also the case for the crystal phase of the CB-C9-CB dimers where<sup>30</sup> the molecules are packed in twisted conformations and the order parameter of the mesogenic units is significantly lower than 1. The very limited variation of the mesogenic order parameter values between the N and  $N_x$  phases suggests that the "orientational frustration" is present in the N phase as well. Accordingly, the molecular packing in the N phase should be similar to that of Fig. 4, left. The important difference between the two phases, from the NMR point of view, is the persistence of the enantio-selective packing in the  $N_x$  phase, which allows the identification of domains of opposite chirality, in contrast to the N phase where the fast inter-conversion between conformations of opposite chirality produces (on the NMR time scale) an achiral medium.

To summarise, in agreement with the findings of a number of previous studies, the results presented here confirm the chirality of the  $N_x$  phase but they call into question the attribution of this chirality to the heliconical distribution of the nematic director according to the twist-bend model. A structural picture is proposed for the consistent interpretation of these results based on the packing of the chiral molecular conformations of the dimers. This picture does not preclude the possibility that, in the absence of the aligning magnetic field, the chiral domains could produce, *via* soft self-assembly, helical structures on a larger length scale under particular surface anchoring.

## Acknowledgements

Funding through the FP7 EU project BIND (Biaxial Nematic Devices, Project no. 216025) is acknowledged.

## References

- 1 P. G. de Gennes and J. Prost, *The Physics of Liquid Crystals*, Oxford University Press, 1995.
- 2 P. H. J. Kouwer, W. F. Jager, W. J. Mijs and S. J. Picken, *Macromolecules*, 2000, **33**, 4336–4342.
- 3 C. Keith, A. Lehmann, U. Baumeister, M. Prehm and C. Tschierske, *Soft Matter*, 2010, **6**, 1704–1721.
- 4 G. Ungar, V. Percec and M. Zuber, *Polym. Bull.*, 1994, **32**, 325–330.
- 5 C. S. P. Tripathi, P. Losada-Pérez, C. Glorieux, A. Kohlmeier, M.-G. Tamba, G. H. Mehl and J. Leys, *Phys. Rev. E: Stat., Nonlinear, Soft Matter Phys.*, 2011, **84**, 041707.
- 6 V. P. Panov, M. Nagaraj, J. K. Vij, Y. P. Panarin, A. Kohlmeier, M. G. Tamba, R. A. Lewis and G. H. Mehl, *Phys. Rev. Lett.*, 2010, **105**, 167801.
- 7 P. A. Henderson and C. T. Imrie, *Liq. Cryst.*, 2011, **38**, 1407–1414.
- 8 M. Cestari, S. Diez-Berart, D. A. Dunmur, A. Ferrarini, M. R. de la Fuente, D. J. B. Jackson, D. O. Lopez, G. R. Luckhurst, M. A. Perez-Jubindo, R. M. Richardson, J. Salud, B. A. Timimi and H. Zimmermann, *Phys. Rev. E: Stat., Nonlinear, Soft Matter Phys.*, 2011, **84**, 031704.
- 9 L. Beguin, J. W. Emsley, M. Lelli, A. Lesage, G. R. Luckhurst, B. A. Timimi and H. Zimmermann, *J. Phys. Chem. B*, 2012, **116**, 7940–7951.
- 10 V. P. Panov, R. Balachandran, J. K. Vij, M. G. Tamba, A. Kohlmeier and G. H. Mehl, *Appl. Phys. Lett.*, 2012, **101**, 234106.
- 11 V. Borshch, Y.-K. Kim, J. Xiang, M. Gao, A. Jákli, V. P. Panov, J. K. Vij, C. T. Imrie, M. G. Tamba, G. H. Mehl and O. D. Lavrentovich, *Nat. Commun.*, 2013, **4**, 2635.
- 12 D. Chen, J. H. Porada, J. B. Hooper, A. Klitnick, Y. Shen, M. R. Tuchband, E. Korblova, D. Bedrov, D. M. Walba, M. A. Glaser, J. E. Maclennan and N. A. Clark, *Proc. Natl. Acad. Sci. U. S. A.*, 2013, **110**, 15931–15936.
- 13 M. G. Tamba, A. Kohlmeier and G. H. Mehl, in *12th ECLC, Book of Abstracts*, Rhodes, Greece, 2013, p. O12.
- 14 R. Balachandran, V. P. Panov, Y. P. Panarin, J. K. Vij, M. G. Tamba, G. H. Mehl and J. K. Song, *J. Mater. Chem. C*, 2014, **2**, 8179–8184.
- 15 E. Gorecka, M. Salamonczyk, A. Zep, D. Pocięcha, C. Welch, Z. Ahmed and G. H. Mehl, arXiv:1410.6369, 2014.
- 16 C. Greco, G. R. Luckhurst and A. Ferrarini, *Phys. Chem. Chem. Phys.*, 2013, **15**, 14961–14965.
- 17 I. Dozov, *Europhys. Lett.*, 2001, **56**, 247–253.
- 18 S. D. Peroukidis, A. G. Vanakaras and D. J. Photinos, *Phys. Rev. E: Stat., Nonlinear, Soft Matter Phys.*, 2011, **84**, 010702.
- 19 S. I. Torgova, L. Komitov and A. Strigazzi, *Liq. Cryst.*, 1998, **24**, 131–142.
- 20 C. Meyer, G. R. Luckhurst and I. Dozov, *Phys. Rev. Lett.*, 2013, **111**, 067801.
- 21 T. Ivšić, M. Vinković, U. Baumeister, A. Mikleušević and A. Lesac, *Soft Matter*, 2014, **10**, 9334–9342.
- 22 M. Gao, Y.-K. Kim, C. Zhang, V. Borshch, S. Zhou, H.-S. Park, A. Jákli, O. D. Lavrentovich, M.-G. Tamba, A. Kohlmeier, G. H. Mehl, W. Weissflog, D. Studer, B. Zuber, H. Gnägi and F. Lin, *Microsc. Res. Tech.*, 2014, **77**, 754–772.
- 23 ESI.†
- 24 K. Czarniecka and E. T. Samulski, *Mol. Cryst. Liq. Cryst.*, 1981, **63**, 205–214.
- 25 D. O. López, N. Sebastian, M. R. de la Fuente, J. C. Martínez-García, J. Salud, M. A. Pérez-Jubindo, S. Diez-Berart,

- D. A. Dunmur and G. R. Luckhurst, *J. Chem. Phys.*, 2012, **137**, 034502.
- 26 D. J. Photinos, E. T. Samulski and H. Toriumi, *J. Chem. Soc., Faraday Trans.*, 1992, **88**, 1875.
- 27 A. Kumar, A. G. Vanakaras and D. J. Photinos, 2015, to be published.
- 28 H. S. Serpi and D. J. Photinos, *Mol. Cryst. Liq. Cryst. Sci. Technol., Sect. A*, 2000, **352**, 205–216.
- 29 P. K. Karahaliou, A. G. Vanakaras and D. J. Photinos, *Liq. Cryst.*, 2005, **32**, 1397–1407.
- 30 K. Hori, M. Iimuro, A. Nakao and H. Toriumi, *J. Mol. Struct.*, 2004, **699**, 23–29.

## Supporting Information

### On the structure of the $N_x$ phase of symmetric dimers: inferences from NMR

Anke Hoffmann<sup>1</sup>, Alexandros G. Vanakaras<sup>2</sup>, Alexandra Kohlmeier<sup>3</sup>,

Georg H. Mehl<sup>3</sup>, Demetri J. Photinos<sup>2</sup>

<sup>1</sup> Department of Inorganic and Analytical Chemistry, University of Freiburg, 79104  
Freiburg, Germany

<sup>2</sup> Department of Materials Science, University of Patras, Patras26504, Greece

<sup>3</sup> Department of Chemistry, University of Hull, Hull, HU6 7RX, UK

*This supporting information file contains details on the NMR measurement and analysis of the measured spectra, a discussion of the influence of rotational viscosity on the NMR spectra and a comparison with the spectra that would be obtained for a hypothetical heliconical configuration of the director according to the twist-bend proposal for the  $N_x$  phase. Preparation of the target material. The DSC of the studied compound is also included.*

#### 1. Details of NMR measurements

**1.1 Experiments.** All spectra were measured on a BrukerAvance 500 NMR spectrometer ( $B_0=11.7\text{ T}$ ,  $\nu_{2H}=76.8\text{ Hz}$ ). Solid echo experiments were performed with  $90^\circ$  pulse length of  $4\ \mu\text{s}$  and a pulse spacing of  $43\ \mu\text{s}$ . For the rotation of the sample a homebuilt probehead with a servomotor was used, triggered from the NMR console (Figure S1a). The sample can be rotated around a fixed axis perpendicular to the magnetic field. Samples were prepared by filling the substance into a 2 cm long glass tube with 4 mm diameter and sealed with a teflon/silicon plug (punched out from a

septum). This tube was then fixed in the middle of a 5mm glass tube making use of teflon band (Figure S1b). The flipping experiments were performed by flipping the sample by  $90^\circ$  around an axis perpendicular to the static magnetic field, data acquisition, and then flipping the sample back to the initial position for the recycle delay (1s). The acquisition starts (earliest) 200 ms after triggering the sample flip, which is the time at which the sample has definitely reached the new orientation. This has been tested extensively with standard samples to get the proper timing and to verify the precision of the angular setting and test the fixation of the sample. Also, this probe has been in use for several years and has been proven to give reliable results for several low molecular weight as well as polymeric liquid crystals.

The spinning experiment spectra shown in Fig 2c were recorded with 100 *rpm* spinning rate about an axis perpendicular to the static magnetic field. Spectra recorded with 6, 60 and 200 *rpm* showed no significant differences at the given temperature. Cooling and heating sequences were run with temperature steps of 1K. After each step the sample was equilibrated for 10 minutes before the start of the acquisition. For the experiments under  $90^\circ$  flipping and under continuous spinning the sample was heated to the isotropic phase and then slowly cooled to the desired temperature. The splittings obtained from different cooling runs agree within an error of less than 1%.

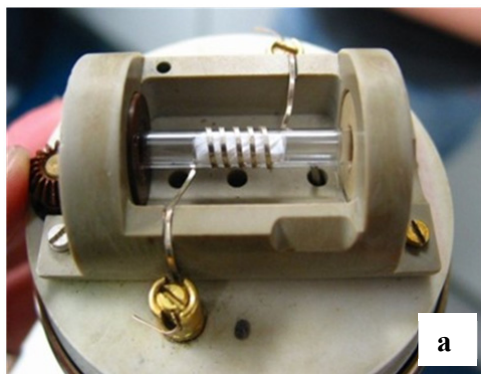
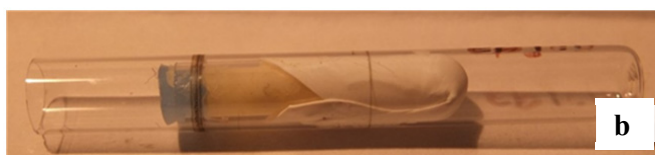


**Figure S1** a.) Probe with a mounted sample tube (not CB-C9-CB). Cog-wheel for rotation can be seen on the left.

b.) Sample tube containing CB-C9-CB.





## 1.2 Analysis of measured spectra.

### *(a) Aligned sample spectra.*

The doubling of each of the quadrupolar peaks of the  $\alpha$ -CD<sub>2</sub> sites in the N<sub>X</sub> phase produces two sub-peaks of different heights and widths. Specifically, the height of the outer sub-peak is appreciably lower but its width is larger than that of the inner sub-peak. The integrated intensity, as it comes out from the direct manual integration in the NMR software is about 10% smaller for the outer peaks. However, this neglects the fact that a part of the outer peaks (the asymmetric ‘foot’ to the middle) lies underneath the inner peaks. When this is taken into account the relative intensities are readily shifted to equality, within the experimental resolution. Furthermore, the simulation of the spectra recorded under continuous rotation, discussed in the next section, is based on summing the two sub-peaks with equal integrated intensities and this yields the essentially exact agreement with the measured spectral distribution of intensity.

### *(b) Spinning sample spectra.*

The experimental spectra obtained under continuous spinning of the sample about an axis perpendicular to the magnetic field were simulated by a powder sum for cylindrical distribution of the nematic directors (i.e. without a scaling factor  $\sin(\beta)$  as for spherical distribution), namely

$$I(t) = \sum_{i=1}^N \cos(2\pi\delta_Q(3\cos^2(\beta_i) - 1)t)$$

Where  $\delta_Q$  is the anisotropy of the (time averaged) quadrupolar coupling tensor; the asymmetry of the tensor is neglected. A set of 200 polar angles  $\beta$ , equally distributed in the range of 0 to  $\pi$ , was used (i.e.  $N=200$ ; a simulation with  $N=400$  showed no significant differences). The spectrum shown in figure 2(c) was simulated as the sum of two cylindrical powder patterns with anisotropies  $\delta_Q$  of 28 kHz and 20.2 kHz – the values of the quadrupolar splitting obtained from the temperature run (Fig 1c). The patterns were added without additional weighting factors (i.e. the two patterns have the same integrated intensity) and scaled to the height of the inner peaks of the experimental spectrum.

### *(c) Simulation of the aligned and 90° –flipped spectra in the N<sub>X</sub> phase.*

In figure S2 we present the experimental NMR spectra of the aligned (red) and of the flipped by 90° with respect to magnetic field samples, (see also fig Fig 2(a) of the

paper). Best fitting curves are also shown for both sets of measured spectra. The line shapes,  $L_{0(90)}(\nu)$ , of these spectra are fitted assuming a superposition of two Lorentzians  $\Lambda(\nu; \delta\nu, w) = w / (\pi(w^2 + (\nu - \delta\nu)^2))$  of the *same integrated intensity*:

$$L_{\theta_{H,n}}(\nu) = \sum_{r=\pm 1} \Lambda\left(\nu; r \frac{\delta\nu_Q(\theta_{H,n})}{2}, w_0(\theta_{H,n})\right) + \Lambda\left(\nu; r \frac{\delta\nu'_Q(\theta_{H,n})}{2}, w'_0(\theta_{H,n})\right) \quad (\text{S.1})$$

Here  $\theta_{H,n} = 0$  or  $90$  denotes the angle between the magnetic field and the director for the aligned and the  $90^\circ$ -flipped samples, respectively.

**Table I.** Best-fit parameters for the simulated spectra with eq (S.1).

$\theta_{H,n}$	$\delta\nu_Q(\theta_{H,n}) / 2$	$w_0(\theta_{H,n})$	$\delta\nu'_Q(\theta_{H,n}) / 2$	$w'_0(\theta_{H,n})$
$0^\circ$	26.958	0.734	21.134	0.380
$90^\circ$	13.545	0.374	10.486	0.260

We note here that for both peaks we have,  $\delta\nu(90) = \delta\nu(0) / 2$  and  $\delta\nu'(90) = \delta\nu'(0) / 2$ , indicating uniaxial ordering in the sample, to within experimental resolution.

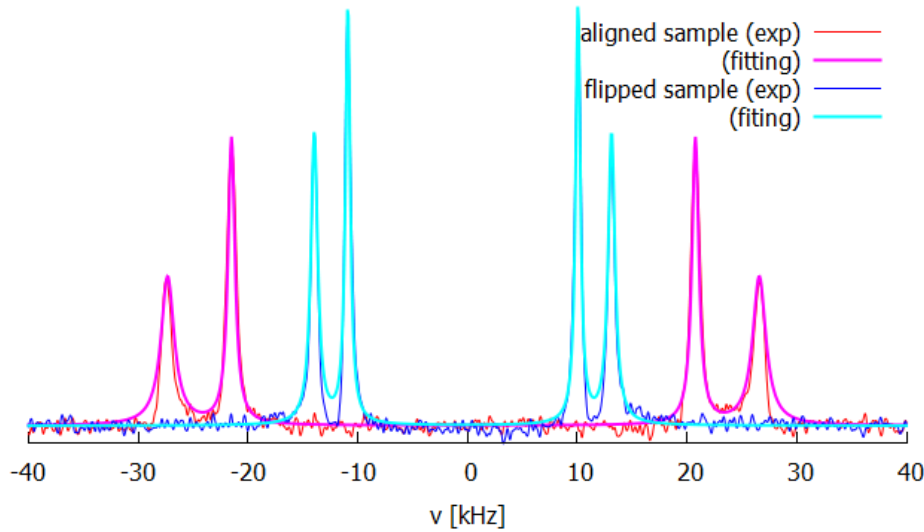


**Figure S2:**  $^2\text{HNMR}$  spectra of the aligned sample (red) and after a flip by  $90^\circ$  with respect to the magnetic field (blue) in the  $N_x$  phase at  $90^\circ\text{C}$ . The thick lines (magenta for the aligned sample and cyan for the  $90^\circ$ -flipped) are simulated spectra assuming Lorentzian line-shapes according to eq(S.1), with the best-fit parameter values listed in Table I.

## 2. The effects of viscosity on the $90^\circ$ -rotated and spinning sample spectra.

At 80°C, spectra recorded under continuous spinning (Figure 2(c)) showed no significant difference when recorded with spinning rates of 6 *rpm*, 60*rpm*, 100 *rpm* and 200 *rpm*. This independence on the spinning rate indicates that a uniform cylindrical distribution of the nematic director is generated by the spinning of the sample and that such distribution is not influenced by hydrodynamic effects, as these would show a dependence on the spinning-rate. Furthermore, the spectra had not relaxed back to equilibrium two hours after the rotation was stopped. Such slow relaxation rates, together with the absence of significant hydrodynamic effects on spinning, are direct implications of the high viscosity of the N<sub>X</sub> phase.

The orientational relaxation times show a relatively rapid variation with temperature within the N<sub>X</sub> phase and a dramatic drop on entering the N phase. Thus, the spectra shown in Figure 2(b), recorded at the temperature of 90°C, are not fully relaxed 10s after the 90° flip. A respective spectrum recorded at 100°C is only partially relaxed after 4s. At 104 °C, the spectra recorded under continuous spinning look different for 1*rpm*, 6*rpm*, 60*rpm*, indicating the onset of appreciable hydrodynamic effects on the director distribution. Lastly, at 106°C, near the onset of the N phase range, the spectra before and after the 90° flip are identical, indicating that the orientation fully relaxes within less than 200 *ms*. Spectra recorded under continuous spinning still show a single splitting for rotation up to 2000 *rpm*; only for rotations of 4000 *rpm* and 5000 *rpm* the spectra get broad. Accordingly, the orientational relaxation time ( $\sim 10^{-3}$ sec) at this temperature is four orders of magnitude faster than the respective time ( $\sim 10$  sec) at the temperature of 90°C in the N<sub>X</sub> phase.

### 3. Spectral line-shape for a hypothetical heliconical configuration with the magnetic field perpendicular to the helix axis

As detailed in the main text the measured 90°-rotated and spinning sample NMR spectra indicate rather directly that the entire sample exhibits a single, uniform, director. Here we present the calculation of the NMR spectrum of a sample assuming that the  $N_X$  phase is a twist-bent nematic presenting a heliconical distribution of the director field. The calculated spectra are then contrasted with the measured spectra. As indicated in the main text, the splitting associated with an  $\alpha$ -C-D bond, is given by the ensemble average:

$$\delta\nu_Q = \nu_Q \left\langle \frac{3}{2} (\hat{H} \cdot \hat{e}_{\alpha-CD})^2 - \frac{1}{2} \right\rangle \quad (\text{S.2})$$

Where  $\hat{H}$  denotes the direction of the magnetic field,  $\hat{e}_{\alpha-CD}$  the direction of the C-D bond and  $\nu_Q = -3q_{CD} / 2$ . In a uniaxial nematic phase, with the director denoted by  $\hat{n}$ , the splitting can be expressed in terms of the “bond order parameter”

$$S_{\alpha-CD}^{(n)} \equiv \left\langle \frac{3}{2} (\hat{n} \cdot \hat{e}_{\alpha-CD})^2 - \frac{1}{2} \right\rangle \quad (\text{S.3})$$

and the orientation of the director relative to the magnetic field as follows:

$$\delta\nu_Q = \nu_Q S_{\alpha-CD}^{(n)} \left( \frac{3}{2} (\hat{H} \cdot \hat{n})^2 - \frac{1}{2} \right) \quad (\text{S.4})$$

With the help of equations (S.2)-(S.4) we can calculate the spectral line-shape for a hypothetical heliconical configuration with the magnetic field perpendicular to the helix axis, obtained by 90-flip of the aligned sample about an axis perpendicular to the magnetic field: In a macroscopic frame where the  $Z$  axis is identified with the helix axis and the direction of the magnetic field (perpendicular to the helix axis) is identified with the  $Y$  axis, the assumed heliconical distribution of the director,  $\hat{n} = (\sin \theta_0 \cos kZ, \sin \theta_0 \sin kZ, \cos \theta_0)$ , would imply the following distribution of the directional term in the rhs of eq (S.4) over the angle  $\varphi = kZ$ ,

$$\frac{3}{2} (\hat{H} \cdot \hat{n})^2 - \frac{1}{2} = \frac{3}{2} (\sin \theta_0 \sin \varphi)^2 - \frac{1}{2} \quad (\text{S.5})$$

In this case we have, according to eq(S.4) a  $\varphi$ -distribution of splittings,

$$\delta\nu_Q(\theta_0, \varphi) = \frac{\nu_Q S_{\alpha-CD}^{(n)}}{2} (3(\sin \theta_0 \sin \varphi)^2 - 1) = \frac{\delta\nu_Q(0)}{2} (3(\sin \theta_0 \sin \varphi)^2 - 1) \quad (\text{S.6})$$



**Figure 3.** NMR spectrum of the 90o-flipped sample (blue) and the corresponding calculated spectra (cyan) for a single, uniformly distributed, director ( $\theta_0 = 0$ ) and for a hypothetical heliconical distribution of the director,  $\mathbf{n} = (\sin \theta_0 \cos kZ, \sin \theta_0 \sin kZ, \cos \theta_0)$ , with values of the “tilt” angle  $\theta_0 = 10^\circ, 20^\circ, 30^\circ$ .

It is clear from equations S.5 to 7 that the measured NMR spectrum can pick up variations of the angle of the director relative to the spectrometer magnetic field and that these variations are manifested as broadening of the spectral lines, in excess to their width at perfect alignment. The resolution of the experimental method sets a lower bound to the extent of variations that can be detected unambiguously on the measured spectra. With the simulation procedure described above we have found that, within the resolution of the experimental spectra, both the aligned sample spectrum and the  $90^\circ$ -flipped spectrum place an upper bound of  $5^\circ$  for possible variations of the angle of the director relative to the magnetic field. Accordingly, if it is assumed that, as a result of a hypothetical heliconical distribution, the director forms a constant angle  $\theta_0$  with the magnetic field, then it is directly deduced from the  $90^\circ$ -flipped spectrum that this angle should be below  $5^\circ$ . Of course variations of such a limited range could also be due to minor fluctuations of the director within the sample, not related to any heliconical distribution. In any case, the upper bound for  $\theta_0 < 5^\circ$ , set by the combined experimental and simulation resolution, is far below the values given for  $5^\circ$  in the literature<sup>2</sup> on the twist-bend nematic phase.

---

<sup>2</sup> (a) V. Borshch, Y.-K. Kim, J. Xiang, M. Gao, A. Jáklí, V. P. Panov, J. K. Vij, C. T. Imrie, M. G. Tamba, G. H. Mehl, and O. D. Lavrentovich, *Nat. Commun.* **4**, 2635 (2013).

(b) D. Chen, J. H. Porada, J. B. Hooper, A. Klitnick, Y. Shen, M. R. Tuchband, E. Korblova, D. Bedrov, D. M. Walba, M. A. Glaser, J. E. Maclennan, and N. A. Clark, *PNAS* **110**, 15931 (2013).

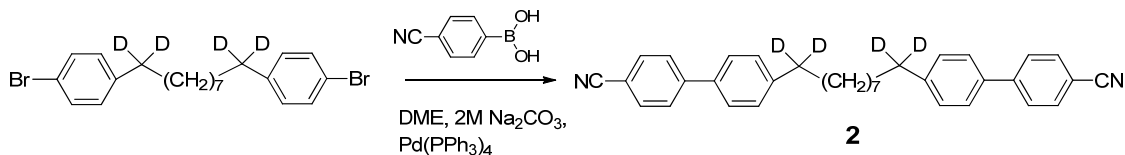
(c) L. Beguin, J. W. Emsley, M. Lelli, A. Lesage, G. R. Luckhurst, B. A. Timimi, and H. Zimmermann, *J. Phys. Chem. B* **116**, 7940 (2012).

(d) C. Meyer, G. R. Luckhurst, and I. Dozov, *Phys. Rev. Lett.* **111**, 067801 (2013).

(e) J. W. Emsley, M. Lelli, A. Lesage, and G. R. Luckhurst, *J. Phys. Chem. B* **117**, 6547 (2013).

(f) C. Greco, G. R. Luckhurst, and A. Ferrarini, *Phys. Chem. Chem. Phys.* **15**, 14961 (2013).

#### 4. Preparation of the target material



**Preparation of 1-d<sub>2</sub>, 9-d<sub>2</sub> -bis([1,1'-biphenyl]-4-carbonitrile) (2):** A solution of **1-d<sub>2</sub>, 9-d<sub>2</sub>-bis-(4-bromophenyl)nonane** (0.70g, 0.0015mol) and), (4-cyanophenyl)boronic acid (0.66g, 0.0045mol) and tetrakis(triphenylphosphine)palladium(0) (0.075g), were dissolved in degassed tetrahydrofuran under an inert atmosphere. After an hour a saturated aqueous solution of sodium carbonate (0.48g) was added drop wise and the reaction is refluxed overnight. The solvent was removed under reduced pressure and the organics separated by silica column chromatography using a mixture of dichloromethane and hexane 1:3 to afford the title compound as a white solid (0.51g, 67%).

<sup>1</sup>H NMR: δ<sub>H</sub> (400 MHz, CD<sub>2</sub>Cl<sub>2</sub>) 7.64 (4H, J = 8.5), 7.59 (4H, J = 8.5) 7.51 (4H, d, J 8.2), 7.29 (4H, d, J 8.16), 1.65-1.55 (4H, m), 1.40-1.20 (10H, m).

<sup>13</sup>C NMR: δ<sub>C</sub> (100 MHz, CDCl<sub>3</sub>) 145.6, 143.8, 132.6, 129.2, 127.5, 127.1, 119.2, 119.0, 110.5, 35.6, 31.4, 31.3, 29.4 (broad C-D), 29.3,

HPLC > 98.6%



### 5. DSC Trace of CB-C9-CB at 10°C min<sup>-1</sup>

